Proceedings of the 10th Brazilian Congress of Thermal Sciences and Engineering – ENCIT 2004
Braz. Soc. of Mechanical Sciences and Engineering – ABCM, Rio de Janeiro, Brazil, Nov. 29 – Dec. 03, 2004

Paper CIT04-0119

CALCULATION OF THE APPARENT PERMEABILITY OF THREE-DIMENSIONAL FIBROUS POROUS MEDIA CONSIDERING INERTIAL EFFECTS

Rodrigo Penha Andrade Rocha
PETROBRAS, CENPES, Eng. de Equipamentos, Cid. Univ., Quadra 7, Prédio 21, S. 2118, Rio de Janeiro, RJ, 21949-900, Brazil
E-mail: rpenha@petrobras.com.br

Manuel Ernani Cruz
Department of Mechanical Engineering, EP/COPPE/UFRJ, CT, Cid. Univ., CP 68503, Rio de Janeiro, RJ, 21945-970, Brazil
E-mail: manuel@serv.com.ufrj.br

Abstract. *In this work, we present an analytical-numerical approach, based on first principles, for the study of inertial incompressible fluid flows through three-dimensional fibrous porous media. Two well-separated spatial scales – the heterogeneity scale and the macroscale – are considered to exist. A multiscale homogenization method for periodic structures, aided by a control-volume-type argument, are then applied to the Navier-Stokes equations to derive the appropriate periodic cell problem. Next, we solve the latter using a Galerkin finite-element formulation, which permits numerical calculation of the apparent permeability of the medium for a given three-dimensional microstructure and Reynolds number. We illustrate the capabilities of our approach by applying it to a benchmark problem, the flow through a square array of unidirectional fibers.*

Keywords*. Apparent permeability, fibrous porous media, Navier-Stokes, homogenization, finite element method.*

1. Introduction

Fluid flows through fibrous porous media take place in many man-made and natural processes like aerosols filtration (Chen, 1955), heat transfer in compact heat exchangers (Hunt and Tien, 1988; Tadrist et al., 2004), air and water clean-up (Pavageau et al., 2000), feeding of microorganisms (Ayaz and Pedley, 1999), chemical reaction catalysis (Bhattacharya et al., 2002), resin transfer molding (Ngo and Tamma, 2001), and dendritic solidification (Brown et al., 2002), to mention some examples.

When dealing with fluid flow through fibrous porous media, the most relevant property of interest is the (tensorial) permeability, which relates the macroscopic pressure drop and volumetric flow rate as stated by the well-known Darcy's law (Kaviany, 1995; Bear, 1972; Darcy, 1856). For creeping flows at the pore scale (or microscale), the permeability depends only on the (generally complex) microstructure of the medium. Furthermore, owing to the large number of heterogeneities, direct simulations of the fluid flow through the intricate paths of real fibrous porous media are prohibitive, and analytical results for the permeability are generally restricted to simple geometric models of the microstructure, as in Sangani and Acrivos (1982).

The phenomenological Darcy's law is theoretically (Keller, 1980) and experimentally (Darcy, 1856; Bear, 1972) obtained only when the inertial effects of the flow are negligible. Nevertheless, for many relevant applications, the hypothesis of creeping flow is not verified, and the permeability is seen to depend on both the microstructure of the medium and the flow Reynolds number (Edwards et al., 1990; Kaviany, 1995; Ghaddar, 1995a, 1995b); as a consequence, a nonlinear filtration law rules the fluid seepage at the macroscale. Because the permeability is not solely a property of the medium for inertial flows, the name "apparent permeability" is used in the literature (Edwards et al., 1990; Ghaddar, 1995a, 1995b), and we will adopt this nomenclature hereafter.

In this work, we present an analytical-numerical approach to predict numerical values for the apparent permeability of three-dimensional fibrous porous media whose microstructures are known *a priori*. The approach is based on a homogenization method for periodic structures (Bensoussan et al., 1978; Hornung, 1997; Auriault, 2001), a control-volume-type argument (Ghaddar, 1995a, 1995b), and the finite element method (Hughes, 1987; Reddy and Gartling, 2001). In section 2, the homogenization equations derived from both the Stokes and Navier-Stokes equations at the pore scale are presented. In section 3, the appropriate cell problem for the inertial-flow case is stated in weak form, and the finite-element solution procedure, based on a classical Galerkin formulation, is described. In section 4, we illustrate the capabilities of our approach by applying it to the benchmark problem of transverse inertial flow through a square array of unidirectional (infinitely long) fibers. Finally, conclusions are given in section 5.

2. Homogenization Equations

Let $\Omega \subset \mathrm{R}^3$ be a bounded domain with boundary $\partial\Omega$; $\Omega = \Omega_f \cup \Omega_s$, where Ω_f is a connected continuous fluid phase, and Ω_s is the dispersed solid phase. The interface between the fluid and solid phases, hereafter indicated respectively by

the subscripts *f* and *s*, is denoted by Γ. The fluid is assumed Newtonian and incompressible, with density ρ and constant dynamic viscosity μ. The solid phase consists of a fixed bed of equal fibers randomly distributed and oriented in Ω (note, however, that the shape and size of the fibers are not restricted by the methodology). A pressure gradient $(\Delta P/L)\mathbf{e}_m$ is imposed over the macroscale L in the x^*_m-direction, m=1,2,3; $\mathbf{e}_m$ is the unit vector parallel to the x^*_m-axis. The multiscale fibrous porous medium Ω is assumed to be periodic at the microscale l in all coordinate directions, with $l << L$, so that the multiscale homogenization method can be applied, and a small parameter $\varepsilon \equiv l/L << 1$ defined. It is important to highlight that periodicity is a mere convenience for analysis, and does not constitute a restriction on the microstructure of the medium (Auriault, 2001).

2.1. Creeping flow

When inertial effects are negligible, the fluid motion is governed by the Stokes equations in Ω_f (we assume summation over repeated indices),

$$\frac{\partial p^*}{\partial x_i^*} = \varepsilon^2 \mu \frac{\partial^2 u_i^*}{\partial x_j^* \partial x_j^*} \quad i = 1,2,3 \quad \text{in } \Omega_f , \tag{1}$$

$$\frac{\partial u_i^*}{\partial x_i^*} = 0 \quad \text{in } \Omega_f , \tag{2}$$

where $\mathbf{x}^* = (x^*_1, x^*_2, x^*_3) \in \mathrm{R}^3$ is the spatial coordinate, $\mathbf{u}^* = (u^*_1, u^*_2, u^*_3)$ is the velocity field, and p^* is the pressure field; the superscript '*' is assigned to dimensional variables. Body forces are neglected. The scaling parameter ε^2 is due to the so-called *homogenization condition*, which requires that the velocity has a nontrivial limit as $\varepsilon \to 0$; in other words, ε^2 scales the viscosity to balance the friction forces on Γ, without exaggerated dissipation (Hornung, 1997).

The medium is assumed to be periodic with period l, and the small parameter $\varepsilon \equiv l/L << 1$ is defined. The medium is partitioned into $N=O(\varepsilon^3)$ periodic cells Q_i^ε, i=1,2,…,N, of characteristic length l, $\Omega = \bigcup_{i=1}^{N} Q_i^\varepsilon$; from the microscopic point of view, each cell Q_i^ε, i=1,2,…,N, is mapped onto a reference periodic cell Q_0 of characteristic length $l_0 = O(l)$. It should be pointed out that the geometry of Q_0 defines the microstructure of the periodic medium completely. Because of the separation of length scales, both the velocity and pressure can be written as a series expansion in powers of ε (Bensoussan et al., 1978; Hornung, 1997; Auriault, 2001):

$$u_i^*(\mathbf{x}^*) = u_i^*(\mathbf{x}^*, \mathbf{y}^*) = \sum_{k=0}^{\infty} \varepsilon^k \, u_i^{(k)}(\mathbf{x}^*, \mathbf{y}^*) , \quad p^*(\mathbf{x}^*) = p^*(\mathbf{x}^*, \mathbf{y}^*) = \sum_{k=0}^{\infty} \varepsilon^k \, p^{(k)}(\mathbf{x}^*, \mathbf{y}^*) , \quad \mathbf{y}^* \equiv \frac{\mathbf{x}^*}{\varepsilon} ; \tag{3}$$

$\mathbf{x}^*$ and $\mathbf{y}^*$ are the dimensional macroscopic (slow) and microscopic (fast) spatial coordinates, respectively. Inserting Eq. (3) into Eqs. (1)-(2), applying the chain rule $\partial/\partial\mathbf{x}^* = \partial/\partial\mathbf{x}^* + (1/\varepsilon)\,\partial/\partial\mathbf{y}^*$, and collecting the terms of order ε^{-1} and ε^0, we respectively obtain

$$\frac{\partial p^{(0)}}{\partial y_i^*} = 0 \quad \rightarrow \quad p^{(0)} = p^{(0)}(\mathbf{x}^*) \quad \text{in } \Omega_f , \tag{4}$$

$$\mu \frac{\partial^2 u_i^{(0)}}{\partial y_j^* \partial y_j^*} = \frac{\partial p^{(1)}}{\partial y_i^*} + \frac{\partial p^{(0)}}{\partial x_i^*} \quad i = 1,2,3 \quad \text{in } \Omega_f . \tag{5}$$

Since $\mathbf{x}^*$ is the macroscopic spatial scale, the pressure field $p^{(0)}$ is the macroscopic pressure field, whose gradient has already been defined:

$$\frac{\partial p^{(0)}}{\partial x_i^*} = \frac{\partial p^{(0)}}{\partial x_m^*} = \frac{\Delta P}{L} \mathbf{e}_m . \tag{6}$$

Consider now the following problem defined in the fluid part of the periodic cell, Q_{0f}: given $m \in \{1, 2, 3\}$, find the periodic fields $K_{im}^*(\mathbf{y}^*)$ and $\Pi_m^*(\mathbf{y}^*)$ that satisfy (Hornung, 1997)

$$\frac{\partial^2 K_{im}^*}{\partial y_j^* \partial y_j^*} = \frac{\partial \Pi_m^*}{\partial y_i^*} - \delta_{im} \quad i = 1,2,3 \quad \text{in } Q_{0f} , \tag{7}$$

$$\frac{\partial K_{im}^*}{\partial y_i^*} = 0 \quad \text{in } Q_{0f} , \tag{8}$$

$$K_{im}^* = 0 \quad i = 1,2,3 \quad \text{on } \Gamma_Q , \tag{9}$$

with periodic boundary conditions on $\partial Q_{0f} \subset \partial Q_0$ (i.e., on the fluid counterpart of the cell's boundary); Γ_Q is the portion of Γ in Q. Substituting the solutions to the cell problem, Eqs. (7)-(9), into Eqs. (5)-(6), we obtain (no sum over m)

$$u_i^{(0)}(\mathbf{x}^*, \mathbf{y}^*) = -\frac{1}{\mu} K_{im}^*(\mathbf{y}^*) \frac{\partial p^{(0)}(\mathbf{x}^*)}{\partial x_m^*} . \tag{10}$$

The phenomenological Darcy's law (Darcy, 1856; Bear, 1972) relates the dimensional superficial velocity **q** and the dimensional pressure gradient **G** for the creeping flow of a viscous incompressible Newtonian fluid through a porous medium by the expression

$$q_i = -\frac{k_{im}^*}{\mu} G_m , \tag{11}$$

where $\mathbf{k}^* = k_{im}^*$ is the permeability tensor, strictly a property of the medium. For the case when both **q** and **G** have the same direction, say, $\mathbf{q} = (q,0,0)$ and $\mathbf{G} = (G,0,0)$, Darcy's law reduces to an algebraic equation, and the permeability tensor **k** reduces to a scalar quantity k ($= k_{11}$); the medium is then said to be isotropic. Averaging now Eq. (10) over the cell domain, we obtain

$$\frac{1}{|Q|}\int_Q u_i^{(0)} d\mathbf{y}^* = -\frac{1}{\mu}\left(\frac{1}{|Q|}\int_Q K_{im}^* d\mathbf{y}^*\right)\frac{\partial p^{(0)}}{\partial x_m^*}, \tag{12}$$

where $|Q| = O(\lambda^3)$ is the volume of the cell Q. Equation (12) is the Darcy's law, obtained via the homogenization method. By inspection of Eqs. (11) and (12), we easily derive the expression for the permeability tensor:

$$k_{im}^* = \frac{1}{|Q|}\int_Q K_{im}^* d\mathbf{y}^* . \tag{13}$$

Thus, by solving the periodic cell problem, Eqs. (7)-(9), for a given microstructure of the medium (defined by the cell geometry), its permeability tensor can be obtained via Eq. (13).

2.2. Inertial flow

The Navier-Stokes equations for the momentum and mass balances in Ω_f are, respectively (we assume summation over repeated indices),

$$\varepsilon\rho\left(\frac{\partial u_i^*}{\partial t^*} + u_j^* \frac{\partial u_i^*}{\partial x_j^*}\right) = -\frac{\partial p^*}{\partial x_i^*} + \varepsilon^2 \mu \frac{\partial^2 u_i^*}{\partial x_j^* \partial x_j^*} \quad i = 1,2,3 \quad \text{in } \Omega_f , \tag{14}$$

$$\frac{\partial u_i^*}{\partial x_i^*} = 0 \quad \text{in } \Omega_f , \tag{15}$$

where t^* is time. The density ρ and viscosity μ are respectively scaled by ε and ε^2, so that all the terms in Eq. (14) have the same importance at the microscale (Hornung, 1997; Marusic-Paloka and Mikelic, 2000), which is our case of interest. Due to the no-slip condition, the velocity $\mathbf{u}^*$ vanishes on the solid-fluid interface Γ.

For a nondimensional formulation of the flow problem, we define the following nondimensional quantities:

$$\mathbf{x} \equiv \frac{\mathbf{x}^*}{d}, \quad t \equiv \frac{t^* U}{d}, \quad \mathbf{u} \equiv \frac{\mathbf{u}^*}{U}, \quad p \equiv \frac{p^* L}{\Delta P\, d}, \quad \mathrm{Re}_U \equiv \frac{\rho U d}{\mu}, \tag{16}$$

where d is the diameter of the fibers, and the velocity scale U is defined as

$$U \equiv \left(\frac{\Delta P\, d}{L\, \rho}\right)^{1/2} . \tag{17}$$

Substituting Eqs. (16)-(17) into Eqs. (14)-(15), we obtain the nondimensional form of the Navier-Stokes equations:

$$\varepsilon\left(\frac{\partial u_i}{\partial t} + u_j \frac{\partial u_i}{\partial x_j}\right) = -\frac{\partial p}{\partial x_i} + \frac{\varepsilon^2}{\mathrm{Re}_U} \frac{\partial^2 u_i}{\partial x_j \partial x_j} \quad i = 1,2,3 \quad \text{in } \Omega_f , \tag{18}$$

$$\frac{\partial u_i}{\partial x_i} = 0 \quad \text{in } \Omega_f . \tag{19}$$

The homogenization theory has already been applied to inertial flows by Mei and Auriault (1991), Marusic-Paloka and Mikelic (2000), and Chen et al. (2001). Mei and Auriault (1991) consider weak inertial effects only, while Marusic-Paloka and Mikelic (2000) and Chen et al. (2001) assume that the inertial terms have the same order of magnitude as

the viscous and pressure terms; in this work we follow the latter approach. Although Marusic-Paloka and Mikelic (2000) and Chen et al. (2001) present rigorous homogenization procedures to obtain the periodic cell and homogenized problems, they do not consider the unsteady effects, which are indeed relevant for moderate Reynolds numbers (Ghaddar, 1995a, 1995b). G. Allaire (Hornung, 1997, chap. 3) states, without proof, that convective and unsteady effects combined can indeed be treated by the homogenization method. The reader is referred to Auriault (2001), and references therein, for details of the homogenization procedure in several fields of physics and engineering.

To consider both convective and unsteady effects, we adopt a widely accepted, physically plausible model based on a control-volume-type argument (Ghaddar, 1995a, 1995b): the contribution of the external boundary conditions on the microscopic flow is solely via the macroscopic pressure gradient, as shown for the creeping flow cell problem. So, based on Eqs. (7)-(9), a periodic cell problem for the unsteady inertial incompressible flow may be inferred for the Navier-Stokes equations of motion: given $m \in \{1, 2, 3\}$ and Re_U, find the (nondimensional) periodic fields $K_{im}(\mathbf{y})$ and $\Pi_m(\mathbf{y})$ that satisfy (hereafter, there is no sum over m)

$$\frac{\partial K_{im}}{\partial t} + K_{jm}\frac{\partial K_{im}}{\partial y_j} - \frac{1}{\mathrm{Re}_U}\frac{\partial^2 K_{im}}{\partial y_j \partial y_j} + \frac{\partial \Pi_m}{\partial y_i} = \delta_{im} \quad i = 1,2,3 \quad \text{in } Q_{0f}\,, \tag{20}$$

$$\frac{\partial K_{im}}{\partial y_i} = 0 \quad \text{in } Q_{0f}\,, \tag{21}$$

$$K_{im} = 0 \quad i = 1,2,3 \quad \text{on } \Gamma_Q\,, \tag{22}$$

with periodic boundary conditions on $\partial Q_{0f} \subset \partial Q_0$. In Eqs. (20)-(22), we have

$$\mathbf{y} \equiv \frac{\mathbf{y}^*}{d}, \quad \mathbf{K} \equiv \frac{\mathbf{K}^*}{d^2}, \quad \mathbf{\Pi} \equiv \frac{\mathbf{\Pi}^*}{d}\,. \tag{23}$$

When inertial effects are not negligible, the pressure gradient and the superficial velocity are not related linearly, and Darcy's law is no longer appropriate. Nevertheless, the linear representation given by Eq. (11) (or, alternatively, by Eq. (12)) can be retained. To account for the nonlinear effects, the tensor $\mathbf{k}$ is made to depend not only on the microstructure, but also on the Reynolds number Re_U; $\mathbf{k}$ is known as the *apparent permeability* (Edwards et al., 1990; Ghaddar, 1995a, 1995b). Because we are dealing with an unsteady flow, our macroscopic (or effective) property – the apparent permeability – must be time-averaged. It can be shown that the nondimensional apparent permeability tensor is given by (Ghaddar, 1995a, 1995b)

$$k_{im} = \frac{1}{T\,|Q|\,\mathrm{Re}_U}\int_0^T\!\!\int_Q K_{im}(\mathbf{y},t)\,d\mathbf{y}dt\,, \tag{24}$$

where $\mathbf{K}$ is the solution of the cell problem given by Eqs. (20)-(22), and T is the characteristic time period of the unsteady flow. Equation (24) defines our task hereafter: the solution of the cell problem – Eqs. (20)-(22)– for $\mathbf{K}(\mathbf{y},t)$, followed by volume and time averaging in order to obtain the apparent permeability $\mathbf{k}$. As mentioned, because the medium is Q-periodic, the geometry of Q defines the medium's microstructure completely. Given that, in general, real fibrous porous media have intricate microstructures, analytical solution of the cell problem in the complex geometry of Q is impractical, requiring thus a numerical solution methodology. In the next section, a Galerkin finite-element formulation for solving the cell problem is presented.

3. Finite-Element Formulation

3.1. Discretization

The first step of the finite-element discretization procedure is to write the problem in its equivalent weak form. Let $L(Q)$ be the space of scalar periodic functions that are square-integrable in Q, and $H(Q)$ the space of scalar periodic functions whose derivatives with respect to y_i, $i = 1,2,3$, belong to $L(Q)$. The weak form of the cell problem, Eqs. (20)-(22), may be written as: given $m \in \{1, 2, 3\}$ and Re_U, find $(K_{1m}, K_{2m}, K_{3m}, \Pi_m) \in ([H(Q)]^3, L(Q))$ such that, for all $(v_1, v_2, v_3, w) \in ([H(Q)]^3, L(Q))$,

$$\int_Q v_i \frac{\partial K_{im}}{\partial t}\,d\mathbf{y} + \int_Q v_i K_{jm}\frac{\partial K_{im}}{\partial y_j}\,d\mathbf{y} + \frac{1}{Re_U}\int_Q \frac{\partial v_i}{\partial y_j}\frac{\partial K_{im}}{\partial y_j}\,d\mathbf{y} - \int_Q \frac{\partial v_i}{\partial y_i}\Pi_m\,d\mathbf{y} = \int_Q v_i \delta_{im} d\mathbf{y}\,, \tag{25}$$

$$\int_Q w\frac{\partial K_{im}}{\partial y_i}\,d\mathbf{y} = 0\,, \tag{26}$$

$$K_{im} = 0 \quad i = 1,2,3 \quad \text{on } \Gamma_Q\,. \tag{27}$$

We next proceed with the domain discretization by constructing a conforming tetrahedral mesh consisting of N_e quadratic elements (10-node tetrahedra); the mesh generation is accomplished using the resourceful third-party software NETGEN 4.0 (Schöberl, 2001). We remark that no selective mesh refinement is carried out at this point; here, we simply use fine uniform meshes. Selective mesh refinement shall be effective to retain precision without exceedingly augmenting the CPU time.

Although the vector $\mathbf{K}_m$ and the scalar Π_m are not rigorously velocity and pressure, respectively, they play such roles in the cell problem, so that finite-elemet discretization of Eqs. (20)-(22) are susceptible to the same numerical restrictions as the ones for the Navier-Stokes problem; hereafter, for convenience, $\mathbf{K}_m$ and Π_m will be referred to as the velocity and pressure fields, respectively. For incompressible flows, equal-order interpolation for both velocity and pressure is not advisable, since it does not guarantee the necessary convergence properties. In order to satisfy the Ladyzhenskaya-Babuska-Brezzi (LBB) consistency condition (Reddy and Gartling, 2001), which assures convergence, we employ Taylor-Hood isoparametric tetrahedral elements in this work. With these elements, the velocity components and the geometry are interpolated quadratically, while the pressure is interpolated linearly. The discrete global velocity and pressure fields can be written as (hereafter the superscript h will be assigned to the discrete quantities):

$$K_{im}^h(\mathbf{y},t) = \sum_{a=1}^{N_U} U_a^i(t)\Psi_a(\mathbf{y}) \qquad \text{and} \qquad \Pi_m^h(\mathbf{y},t) = \sum_{a=1}^{N_P} P_a(t)\Phi_a(\mathbf{y})\,. \tag{28}$$

In Eq. (28), ${U^i}_a$ is the unknown value of the i-component of the velocity field ${\mathbf{K}_m}^h$ at node a, $a = 1,\ldots, N_U$; N_U is the number of unknown values (degrees-of-freedom) of ${K_{im}}^h$. Analogously, P_a is the unknown value of the pressure field ${\Pi_m}^h$ at node a, $a = 1,\ldots, N_P$, and N_P is the number of unknown values of ${\Pi_m}^h$. The quadratic and linear finite-element interpolation functions at node a of a 10-node tetrahedron are $\Psi_a(\mathbf{y})$ and $\Phi_a(\mathbf{y})$, respectively. As usual in a Galerkin formulation, the weighting functions are approximated by the shape functions themselves (Reddy and Gartling, 2001):

$$v_i^h(\mathbf{y}) = \Psi_a(\mathbf{y})\,, \quad w^h(\mathbf{y}) = \Phi_a(\mathbf{y})\,. \tag{29}$$

Because the velocity $\mathbf{K}_m$ is quadratically interpolated, it must be calculated at all the ten nodes of every quadratic tetrahedron, while the linearly-interpolated pressure is calculated at the four vertices only. As a consequence, $N_U > N_P$ in general (because of the no-slip condition, ${U^i}_k$ do not include the nodes at which ${K_{im}}^h$ is known, and, thus, we may find $N_U < N_P$ for some coarse meshes).

The weak form of the cell problem, Eqs. (25)-(27), can now be stated in its discrete form: given $m \in \{1, 2, 3\}$ and Re_U, find $({K_{1m}}^h, {K_{2m}}^h, {K_{3m}}^h, {\Pi_m}^h) \in ([H^h(Q)]^3, L^h(Q))$ such that, for all $({v_1}^h, {v_2}^h, {v_3}^h, w^h) \in ([H^h(Q)]^3, L^h(Q))$,

$$\int_{Q^h} v_i^h \frac{\partial K_{im}^h}{\partial t}\,d\mathbf{y} + \int_{Q^h} v_i^h K_{jm}^h \frac{\partial K_{im}^h}{\partial y_j}\,d\mathbf{y} + \frac{1}{\mathrm{Re}_U}\int_{Q^h} \frac{\partial v_i^h}{\partial y_j}\frac{\partial K_{im}^h}{\partial y_j}\,d\mathbf{y} - \int_{Q^h} \frac{\partial v_i^h}{\partial y_i}\Pi_m^h\,d\mathbf{y} = \int_{Q^h} v_i^h \delta_{im}\,d\mathbf{y}\,, \tag{30}$$

$$\int_{Q^h} w^h \frac{\partial K_{im}^h}{\partial y_i}\,d\mathbf{y} = 0\,, \tag{31}$$

$$K_{im}^h = 0 \quad i = 1,2,3 \quad \text{on } \Gamma_Q\,; \tag{32}$$

Q^h is the finite-element mesh, i.e., the union of all tetrahedra τ_e, $e = 1,\ldots,N_e$. The spaces $L^h(Q)$ and $H^h(Q)$ are defined as

$$L^h(Q) = L(Q) \cap Y_1(\tau_e)\,, \quad H^h(Q) = H(Q) \cap Y_2(\tau_e)\,, \tag{33}$$

where $Y_p(\tau_e)$ is the space of all polynomials of degree p defined over element τ_e. Substituting Eqs. (28)-(29) into the discrete cell problem, Eqs. (30)-(32), and performing numerical integration, we are led to the following nonsymmetric system of nonlinear algebraic equations (Ghaddar, 1995a, 1995b):

$$\mathbf{M}\frac{d}{dt}\mathbf{U}^i \;+\; \mathbf{C}(\mathbf{U}^i)\cdot\mathbf{U}^i \;=\; -\frac{1}{\mathrm{Re}_U}\mathbf{A}\cdot\mathbf{U}^i \;+\; \mathbf{D}_i^T\cdot\mathbf{P} \;+\; \mathbf{M}\cdot\mathbf{f}_i \qquad i = 1,2,3\,, \tag{34}$$

$$\mathbf{D}_i\cdot\mathbf{U}^i \;=\; \mathbf{0}\,, \tag{35}$$

where $\mathbf{A}$ is the symmetric discrete Laplacian operator, $\mathbf{D}_i$ is the discrete divergence operator, $\mathbf{M}$ is the mass matrix, the vector $\mathbf{f}_i = \delta_{im}$ represents the nondimensional external pressure gradient, and $\mathbf{C}(\mathbf{U}^i)$ is the nonsymmetric *nonlinear* convective operator, which depends on the solution $\mathbf{U}^i$; the vectors $\mathbf{U}^i$ and $\mathbf{P}$ comprise, respectively, the i-component of the velocity and pressure nodal unknowns (see Eq. (28)). To satisfy Eq. (32), we impose null velocity at every node on the interface Γ_Q; these known nodal velocity values are not part of the unknown vector $\mathbf{U}^i$.

For a time-stepping solution procedure, the viscous term is integrated through an implicit backward scheme, and the nonlinear term is treated explicitly by the 3rd-order Adams-Bashforth scheme, leading to (Ghaddar, 1995a, 1995b):

$$\left(\frac{1}{\mathrm{Re}_U}\mathbf{A} + \frac{1}{\Delta t_n}\mathbf{M}\right)\cdot\mathbf{U}_{n+1}^i - \mathbf{D}_i^T\cdot\mathbf{P}_{n+1} = \frac{1}{\Delta t_n}\mathbf{M}\cdot\mathbf{U}_n^i - \sum_{p=0}^{2}\alpha_p\mathbf{C}(\mathbf{U}_{n-p}^i)\cdot\mathbf{U}_{n-p}^i + \mathbf{M}\cdot\mathbf{f}_i \qquad i = 1,2,3\,, \tag{36}$$

$$\mathbf{D}_i \cdot \mathbf{U}_{n+1}^i = \mathbf{0}\,, \tag{37}$$

where the subscript n refers to the nth iteration, Δt_n is the time step, and $(\alpha_0,\alpha_1,\alpha_2)$ are coefficients which depend on the last three time steps, see Ghaddar (1995a, 1995b) for the corresponding explicit functional expressions. In the next subsection, we detail the solution procedure of the system given by Eqs. (36)-(37).

3.2. Solution of the nonlinear system

This subsection is devoted to the solution of the nonsymmetric system of nonlinear algebraic equations, Eqs. (36)-(37), in order to obtain the unknown values of the three components of the velocity field and the pressure field, represented by vectors $\mathbf{U}^1$, $\mathbf{U}^2$, $\mathbf{U}^3$ and $\mathbf{P}$, respectively. An operator splitting method is used, such that the original nonsymmetric system of nonlinear equations is broken into the following *symmetric* system of decoupled *linear* equations (Ghaddar, 1995a, 1995b):

$$\mathbf{H} \cdot \widetilde{\mathbf{U}}_{n+1}^i = \mathbf{D}_i^T \cdot \mathbf{P}_n + \frac{1}{\Delta t_n}\mathbf{M} \cdot \mathbf{U}_n^i - \sum_{p=0}^{2} \alpha_p \mathbf{C}(\mathbf{U}_{n-p}^i) \cdot \mathbf{U}_{n-p}^i + \mathbf{M} \cdot \mathbf{f}_i \qquad i = 1,2,3\,, \tag{38}$$

$$\mathbf{E} \cdot \mathbf{P}_{n+1} = \mathbf{E} \cdot \mathbf{P}_n - \frac{1}{\Delta t_n}\mathbf{D}_i \cdot \widetilde{\mathbf{U}}_{n+1}^i\,, \tag{39}$$

$$\mathbf{U}_{n+1}^i = \widetilde{\mathbf{U}}_{n+1}^i + \Delta t_n \mathbf{M}^{-1} \cdot \mathbf{D}_i^T (\mathbf{P}_{n+1} - \mathbf{P}_n)\,, \tag{40}$$

where $\widetilde{\mathbf{U}}^i$ is the intermediate velocity field, and $\mathbf{H}$ and $\mathbf{E}$ are, respectively, the Helmholtz and Poisson operators, defined as

$$\mathbf{H} \equiv \frac{1}{\mathrm{Re}_U}\mathbf{A} + \frac{1}{\Delta t_n}\mathbf{M}\,, \quad \mathbf{E} \equiv \mathbf{D}_i \cdot \mathbf{M}^{-1} \cdot \mathbf{D}_i^T\,; \tag{41}$$

summation over the repeated index i is assumed.

It should be pointed out that, to avoid prohibitive memory consumption when refined meshes are used, we do not assemble the global matrices; instead, we solve Eqs. (38)-(40) at the elemental (or local) level, which does not require a direct solution method. Because the coefficient matrices in Eqs. (38)-(40) are all symmetric positive definite, we employ the *conjugate gradient method* (Shewchuk, 1994); the nonsymmetric matrix $\mathbf{C}$ is treated explicitly, and so it does not operate as a coefficient matrix. As the operations are carried out at the elemental level, the mass matrix $\mathbf{M}$ cannot be inverted directly, and we would thus have to use a nested conjugate gradient loop for solving Eq. (39), and one simple conjugate gradient loop for solving Eqs. (38) and (40).

Instead of using the mass matrix $\mathbf{M}$, we replace it by the diagonal lumped mass matrix $\mathbf{L}$, defined locally in the tetrahedral element τ_e as (Ghaddar, 1995a, 1995b)

$$L_j^e \equiv M_{jj}^e \frac{|\,\tau_e\,|}{\mathrm{tr}\,\mathbf{M}^e}\,, \tag{42}$$

where $|\,\tau_e\,|$ is the volume of tetrahedron τ_e. The substitution of the mass matrix $\mathbf{M}$ by the diagonal matrix $\mathbf{L}$ eliminates the need for a nested conjugate gradient loop for solving Eq. (39), and leads to a single loop; besides, Eq. (40) does not require any iterative solution procedure. The approximation given by Eq. (42) is very attractive and suitable for our purposes, because not only computation time is drastically reduced, but also the associated error vanishes completely when a steady-state solution is achieved (Ghaddar, 1995a, 1995b).

For a more efficient time-stepping solution procedure, the time step of the subsequent iteration n+1 is calculated based on the Courant condition for the current iteration n. For every edge h_k (k = 1,2,…,6) of every tetrahedron τ_e (e = 1,2,…,N_e), the Courant number is defined as (Ghaddar, 1995a)

$$Cr = \frac{u\,\Delta t_n}{h_k / 2}\,, \tag{43}$$

where u is the projection of the velocity vector on the edge h_k. In the mesh, there is a certain edge of a certain tetrahedron for which the Courant number is a maximum, Cr_{max}. For the finite-difference scheme adopted here, we must have $Cr_{max} < 0.723$ in order to guarantee a stable solution (Ghaddar, 1995a). If this criterion is not observed, the entire calculation carried out at iteration n is abandoned, and a new time step Δt_n, calculated with $Cr = 0.5$, is considered:

$$\Delta t_n = 0.5\frac{h_k}{2u}\,. \tag{44}$$

Ghaddar (1995a, 1995b) states that the choice $Cr = 0.5$ provides stable solutions for the range of moderate Reynolds numbers considered in this paper. For the next iteration n+1, if the stability criterion ($Cr_{max} < 0.723$) is verified, the same time step is used, provided it is larger than the one given by Eq. (44); otherwise, the value calculated by Eq. (44) is used.

3.3. Calculation of the apparent permeability

Once Eqs. (38)-(40) are solved, and the nodal values of the velocity and pressure fields obtained, we are able to calculate the numerical (tensorial) apparent permeability $\mathbf{k}^h$. In this paper, we are only concerned with the most relevant permeability entries k_{mm}; entry k_{mm} relates the x_m-component of the superficial velocity to the external pressure gradient imposed in the x_m-direction. Choosing $m = 1$, the expression for the numerical (scalar) apparent permeability, from Eq. (24), is

$$k^h \equiv k_{11}^h = \frac{1}{T\,|Q|\,\mathrm{Re}_U} \int_0^T \int_{Q^h} K_{11}^h(\mathbf{y},t)\, d\mathbf{y}\, dt \ . \tag{45}$$

Besides Eq. (45), by means of which we calculate k^h via 8-point Gaussian quadrature, the following alternative expressions may be used to evaluate k^h (Ghaddar, 1995a, 1995b):

$$k^h = \frac{1}{T\,|Q|\,\mathrm{Re}_U^2} \int_0^T \left(\mathbf{U}^i\right)^T \cdot \mathbf{A} \cdot \mathbf{U}^i \, dt \tag{46}$$

and

$$k^h = \frac{1}{T\,\mathrm{Re}_U} \int_0^T 1^T \cdot \mathbf{M} \cdot \mathbf{U}^1 dt \ , \tag{47}$$

where, again, summation over the repeated index i is assumed. Equations (46)-(47) are derived from Eqs. (25)-(26), and may be used interchangeably to evaluate the apparent permeability (a useful check for the implementation).

4. Preliminary Numerical Results

The main objectives of this section are, first, to illustrate the capabilities of the approach exposed in sections 2-3, and, second, to validate our implementation by comparing our numerical results to those of Ghaddar (1995a, 1995b). Ghaddar (1995a, 1995b) was limited to two-dimensional problems, and computed, among other quantities, the apparent permeability for the *flow across a square array of infinitely long circular cylinders*. We remark that, despite the simplicity of the two-dimensional problem considered in this section, our calculation is truly three-dimensional, such that our numerical methodology should be capable of solving more complex and realistic problems.

In the work of Ghaddar (1995a, 1995b), the geometry of the periodic cell is composed of a circle of unitary diameter placed at the center of a square of side $\lambda = (1/2)(\pi/c)^{1/2}$; the cylindrical fiber (solid phase) is thus represented by the circle, while the fluid phase is represented by the area inside the square and outside the circle. The external pressure gradient is oriented in the y_1-direction, perpendicular to the fiber's axis. A schematic of the 2-D periodic cell configuration is presented in Fig. (1). In order to simulate this two-dimensional problem, our three-dimensional periodic cell is composed of a circular cylinder of unitary diameter (the solid fiber) placed at the center of a cube, in such a way that the cylinder's axis is parallel to four of the cube's faces, and thus perpendicular to the other two. The planes of the cylinder's bases coincide with those of the two perpendicular faces. Obviously, both the cube's edge and the cylinder's height have the same length $\lambda = (1/2)(\pi/c)^{1/2}$. Periodicity is imposed on every pair of opposing faces, edges and vertices of the cube, so as to reproduce the 2-D square array of cylinders. The external pressure gradient is imposed in the y_1-direction, perpendicular to the cylinder's axis (which is parallel to the y_3-direction, out of the plane of Fig. (1)).

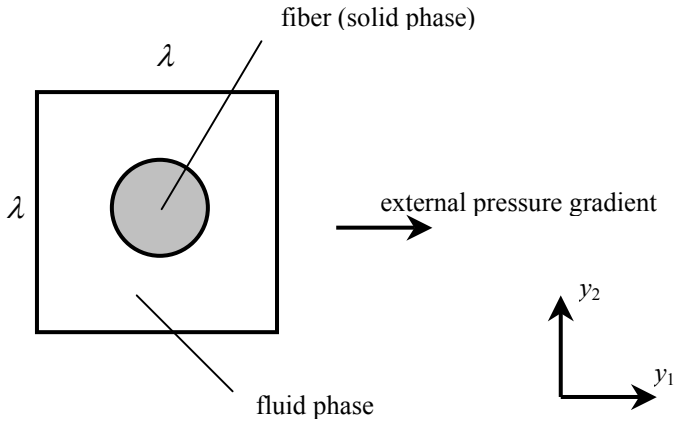

Figure 1. Schematic of the 2-D periodic cell for the flow across a square array of infinitely long cylindrical fibers.

The fluid phase domain is discretized by a uniform tetrahedral finite-element mesh with nominal mesh spacing set to $h_0 = \lambda/16$. The integrity and quality of the mesh are guaranteed by the internal checks and procedures performed by NETGEN 4.0. The relative tolerance for stopping each conjugate gradient iteration is 10^{-5}, and the entire calculation algorithm stops when the relative numerical discrepancy between the permeability results obtained with Eqs. (46) and (47) is less than 10^{-4}; the value calculated using Eq. (46) approaches the one calculated using Eq. (47) as the solution approaches the steady-state.

In Tab. (1) we present our numerical results for the apparent permeability, k^h, and the numerical results obtained by Ghaddar (1995a, 1995b), k_G, for the solid volume fraction $c = 0.2$ and three values of the input Reynolds number, Re_U. We remark that, since Re_U is defined in terms of the pressure-gradient-based velocity scale U, it is not the 'real' Reynolds number of the flow; the latter may be obtained *a posteriori*, as shown by Ghaddar (1995a, 1995b). The relative discrepancy δ, given by

$$\delta = \frac{|k^h - k_G|}{k_G} \times 100\%, \tag{48}$$

is also presented.

Table 1. Our numerical results, k^h, and those obtained by Ghaddar (1995a, 1995b), k_G, for the apparent permeability of the square array of unidirectional (infinitely long) circular cylindrical fibers, for the solid volume fraction $c = 0.2$ and three values of Re_U. The relative discrepancy δ between k^h and k_G is also shown.

Re_U	k^h	k_G	δ
17.2	0.06677	0.06602	1.14%
25.2	0.06231	0.06141	1.47%
30.0	0.06042	0.06055	0.21%

By inspection of the results in Tab. (1), we verify the very good agreement between k^h and k_G. In fact, the relative discrepancy δ is less than 1.5% for all cases, indicating the correctness of our calculation algorithm and implementation. The observed discrepancy will certainly decrease, without an exaggerated increase in CPU time, when selectively refined meshes are used.

From a physical point of view, for a fixed solid volume fraction, the results in Tab. (1) show that the apparent permeability decreases as the Reynolds number increases. This behavior may be explained by the fact that the drag force (which is related to the inverse of the permeability) is higher for more pronounced inertial effects.

5. Conclusions

In this work-in-progress paper, we have presented an analytical-numerical approach, based on first principles, for the calculation of the apparent permeability of three-dimensional fibrous porous media whose microstructures are known *a priori*. A multiscale homogenization method for periodic structures has been applied to the Stokes and unsteady Navier-Stokes equations defined over the original multiscale medium. In the latter case, in view of the difficulties of the homogenization method in handling the combined effects of convection of momentum and unsteadiness, a control-volume-type argument is also employed. The appropriate cell problem for the inertial-flow case, derived from the homogenization procedure, has been suitably discretized and solved, based on a classical Galerkin finite element formulation. Finally, the capabilities of the approach are illustrated for a simple model microstructure, where the fibers are represented by infinitely long circular cylinders arranged in a square array, successfully verifying the calculation procedure.

In future work, given the rigor and flexibility of the approach, we intend to apply the present methodology to more realistic three-dimensional microstructures of porous media. We believe new relevant results for the apparent permeability of such media will be obtained.

6. Acknowledgements

The authors would like to gratefully acknowledge the support of CNPq (Grant nº 500086/2003-6) and FAPERJ (Grant Bolsa Nota 10 nº E-26/150854/2002). The authors would also like to thank Dr. J. Schöberl, from Johannes Kepler Universität Linz, Austria, for freely licensing NETGEN 4.0 for academic use.

7. References

Auriault, J.-L., 2001, "Homogénéisation", UJF, INPG, Grenoble, France.

Ayaz, F. and Pedley, T.J., 1999, "Flow through and particle interception by an infinite array of closely-spaced circular cylinders", Eur. J. Mech. B/Fluids, Vol. 18, No. 2, pp. 173-196.

Bear, J., 1972, "Dynamics of fluids in porous media", Dover Publications, Inc., New York.

Bensoussan, A., Lions, J.-L. and Papanicolaou, G.C., 1978, "Asymptotic analysis for periodic structures", North-Holland, Amsterdam.

Bhattacharya, A., Calmidi, V.V. and Mahajan, R.L., 2002, "Thermophysical properties of high porosity metal foams", Int. J. Heat Mass Transfer, Vol. 45, pp. 1017-1031.

Brown, S.G.R., Spittle, J.A., Jarvis, D.J. and Walden-Bevan, R., 2002, "Numerical determination of liquid flow permeabilities for equiaxed dendritic structures", Acta Materialia, Vol. 50, pp. 1559-1569.

Chen, C.Y., 1955, "Filtration of aerosols by fibrous media", Chem. Rev., Vol. 55, pp. 595-623.

Chen, Z., Lyons, S.L. and Qin, G., 2001, "Derivation of the Forchheimer law via homogenization", Transport in Porous Media, Vol. 44, pp. 325-335.

Darcy, H., 1856, "Les fontaines publiques de la ville de Dijon", Victor Dalmont, Paris.

Edwards, D.A., Shapiro, M., Bar-Yoseph, P. and Shapira, M., 1990, "The influence of Reynolds number upon the apparent permeability of spatially periodic arrays of cylinders", Phys. Fluids A, Vol. 2, No. 1, pp. 45-55.

Ghaddar, C.K., 1995a, "Parallel analytico-computational methods for multicomponent media: Application to thermal composites and porous-media flows", Ph.D. thesis, Massachusetts Institute of Technology.

Ghaddar, C.K., 1995b, "On the permeability of unidirectional fibrous media: A parallel computational approach," Phys. Fluids, Vol. 7, No. 11, pp. 2563-2586.

Hornung, U., 1997, "Homogenization and porous media", Springer-Verlag New York, Inc., New York.

Hughes, T.J.R., 1987, "The finite element method: linear static and dynamic finite element analysis", Prentice Hall, Englewood Cliffs, New Jersey.

Hunt, M.L. and Tien, C.L., 1988, "Effects of thermal dispersion on forced convection in fibrous media", Int. J. Heat Mass Transfer, Vol. 31, No. 2, pp. 301-309.

Kaviany, M., 1995, "Principles of Heat Transfer in Porous Media", 2nd ed., Springer-Verlag New York, Inc., New York.

Keller, J.B., 1980, "Darcy's law for flow in porous media and the two-space method". In: "Nonlinear partial differential equations in engineering and applied sciences", Lecture notes on pure and applied mathematics, Eds. Sternberg, R.L., Kalinowski, A.J. and Papadakis, J.S., Dekker, New York, pp. 429-443.

Marusic-Paloka, E. and Mikelic, A., 2000, "The derivation of a nonlinear filtration law including the inertia effects via homogenization", Nonlinear Analysis, Vol. 42, pp. 97-137.

Mei, C.C. and Auriault, J.-L., 1991, "The effect of weak inertia on flow through a porous medium", J. Fluid Mech., Vol. 222, pp. 647-663.

Ngo, N.D. and Tamma, K.K., 2001, "Microscale permeability predictions of porous fibrous media", Int. J. Heat Mass Transfer, Vol. 44, pp. 3135-3145.

Pavageau, M., Le Coq, L., Mabit, J. and Solliec, C., 2000, "About the applicability of commonly used pressure-flow models to plane single-layer filters of activated carbon fabric", Chem. Engng. Sci., Vol. 55, pp. 2699-2712.

Reddy, J.N. and Gartling, D.K., 2001, "The finite element method in heat transfer and fluid dynamics", 2nd ed., CRC Press, Boca Raton, Florida.

Sangani, A.S. and Acrivos, A., 1982, "Slow flow past periodic arrays of cylinders with application to heat transfer", Int. J. Multiphase Flow, Vol. 8, pp. 193-206.

Schöberl, J., 2001, "NETGEN – 4.0", Numerical and Symbolic Scientific Computing, Johannes Kepler Universität Linz, Austria.

Shewchuk, J.R., 1994, "An introduction to the conjugate gradient method without the agonizing pain", School of Computer Science, Carnegie Mellon University, Pittsburgh, Pennsylvania.

Tadrist, L., Miscevic, M., Rahli, O. and Topin, F., 2004, "About the use of fibrous materials in compact heat exchangers", Exper. Thermal Fluid Sci., Vol. 28, pp. 193-199.

8. Copyright Notice